Formation of a Five-Seven Pair Couple Defect in Double-Walled Carbon Nanotubes under Bending Deformation

メタデータ	言語: eng
	出版者:
	公開日: 2017-10-03
	キーワード (Ja):
	キーワード (En):
	作成者:
	メールアドレス:
	所属:
URL	https://doi.org/10.24517/00010904

Formation of a five-seven pair couple defect in double-walled carbon nanotubes under bending deformation

Kei Wako,[a)] Isamu Okada, Masaru Tachibana, and Kenichi Kojima
Graduate School of Integrated Science, Yokohama City University, 22-2 Seto, Kanazawa-ku, Yokohama 236-0027, Japan

Tatsuki Oda
Graduate School of Natural Science and Technology, Kanazawa University, Kakuma-machi, Kanazawa 920-1192, Japan

Simulations of double-walled carbon nanotubes under bending deformation using the tight-binding molecular dynamics method were carried out. Five- and seven-membered ring pair defects were formed after emission of several atoms from the tube structure. These defect pair couples have different structures corresponding to the number of emitted atoms and stabilize the resulting nanotubes. Our results imply that the defect pair couples represent one of the potential origins of the experimentally observed plastic deformations that have been shown to occur in double-walled carbon nanotubes. The various defects obtained by the simulations are discussed in relation to other defect types. © *2007 American Institute of Physics*. [DOI: 10.1063/1.2821247]

I. INTRODUCTION

Since the discovery of carbon nanotubes,[1] they have become one of the most intensively studied materials, and due to their mechanical and electronic properties they are promising building blocks for the construction of nanosized electronic and electromechanical devices. At temperatures less than or equal to room temperature, the excellent mechanical resistance of carbon nanotubes to bending deformation or tensile strain has already been observed experimentally and studied theoretically.[2–5] At high temperatures, however, plastic deformation and the formation of structural defects have been shown both experimentally and theoretically as well. For example, Huhtala *et al.* have carried out computer simulations with regard to the bending of single-walled nanotubes (SWNTs)[6] and their results indicated that plastic deformation occurred. Tensile strain has also been reported as a cause for structural defects.[7–9]

In theoretical approaches the simple structure of SWNTs should confer an advantage to easily control electronic properties of such nanotubes; however, there are shortcomings in terms of mechanical stiffness. Indeed, the one-dimensionality of SWNTs may deteriorate by the presence of only a few defects in the wall structure. The structure of double-walled carbon nanotubes (DWNTs) is not as complex as that of multiwalled carbon nanotubes (MWNTs) and is more rigid than SWNTs. Due to this situation, DWNTs are considered to be attractive materials with regard to structural integrity and subsequently, high-quality DWNTs have been synthesized and investigated with Raman optical measurements and by transmission electron microscopy.[10–15]

Recently it was found that application of electric current resulted in plastic deformation of DWNTs that had previously been bent elastically via mechanical stress.[16] There have been few studies with regard to plastic deformation and the formation of structural defects in DWNTs, yet it is important to understand the types of defects that may form. The present study was carried out to investigate the structural defects of DWNTs under bending deformation. Following emission of several atoms, two five- and seven-membered ring pairs were formed. We call this structural defect a 5-7 pair couple defect, and DWNTs that contain this 5-7 pair defect were found to be more stable under bending deformation conditions. Five-seven pair defects have been previously observed at the connection junctions of nanotubes which had different chiralities and almost the same diameter.[17] Recently, Mori *et al.* studied plastic deformation in SWNTs and showed a slightly different type of 5-7 pair couple defect in which the number of atoms in the nanotube did not change.[18]

II. METHOD

The nanotube used in this study is a $(3,3)@(8,8)$ DWNT possessing an inner tube chirality of $(3,3)$ and an outer tube chirality of $(8,8)$. Such a pair of $(3,3)$ and $(8,8)$ nanotubes has an interwall distance that is close to the graphite interlayer distance of 3.35 Å. The diameters of the inner and outer tubes and the interwalled distance are 4.07, 10.86, and 3.39 Å, respectively. A recent potential energy calculation for DWNTs shows that the potential energy curve with respect to interlayer distance has a minimum between 3.3 and 3.5 Å.[19] The DWNT has 10 units of armchair nanotubes along the axial direction, which amounts to 23.4 Å and 440 atoms in the system. The initial atomic configuration was constructed by bending along an arc with a curvature radius of 30 Å, as shown in Fig. 1(a). The radii of the nanotubes are relatively smaller than that of most observed DWNTs, while the diameter of 3 Å has been reported in MWNTs.[20]

Simulations were carried out by employing the tight-binding molecular dynamics method in which the potential parameters developed by Xu *et al.* were used.[21] This set of parameters was used because they aptly describe the dy-

---
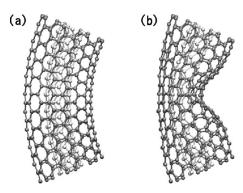[a)]Electronic mail: s045913a@yokohama-cu.ac.jp.

FIG. 1. (a) Initial atomic configuration of DWNT with a curvature radius of 30 Å and (b) final state after 3.0 ps. The inner and outer tube have chiralities of $(3,3)$ and $(8,8)$, respectively.
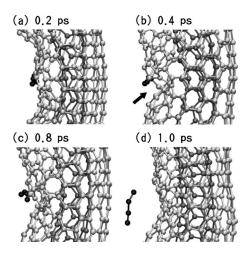

FIG. 2. Snapshots of the process for the cluster emission at an initial temperature of 200 K. The dark gray, light gray, and black atoms denote inner tube, outer tube, and emitted atoms, respectively. The arrow in (b) denotes a hole which appeared along the circumference of the tube. The values in the figures denote the simulation time of each snapshot.

namic and elastic properties of nanotubes with good accuracy and reliability. Although these parameters are not as accurate as the more time-consuming quantum-mechanical methods,[22,23] it is very useful for semiquantitative estimates and for explorations of large numbers of calculations over large portions of the potential energy landscape. The Verlet algorithm[24] was used to integrate the equations of motion with a time step of 1.0 fs for an overall time of 3.0 ps. During simulations the carbon atoms at both ends of the tube were fixed in their initial positions.

To assign temperatures to a system, we introduced an initial distortion and an initial kinetic energy. For the latter, which is expressed with an initial temperature, each carbon atom was assigned an initial velocity according to three types of random number distributions (seeds 1, 2 and 3). The system was studied over an initial temperature range of 0 K to 5000 K in steps of 200 K by employing the microcanonical ensemble. In this work, the initial temperatures were used for labeling the respective simulations. The system temperature during the simulation was generated from the given initial kinetic energy and the deformation potential. The minimum energy configurations at zero temperature were obtained by using a quench method.

When the simulation was carried out without the initial temperature, only thermal vibration occurred and no bond breakage was caused, as shown in Fig. 1(b). The system temperature was increased by the initial distortion, and the average temperature after 0.5 ps was estimated to be 1055 K. In our simulations, the average temperature after 0.5 ps was around 1055 K plus the initial temperature.

III. RESULTS AND DISCUSSIONS

A. Overview of simulations

Simulations were mainly performed at the various initial temperatures using seed 1. Various phenomena (bond breakage, atom emission, and defect formation) occurred depending on the given temperature. When the simulation was performed with an initial temperature of 200 K, four atoms were emitted from inside of the arc with a curvature radius of 30 Å, as shown in Fig. 2. As a result, two 5-7 pair defects were formed as shown in Fig. 3(b). The average temperature was 1262 K after 0.5 ps. In the case where the initial temperature was 2000 K, eight atoms were emitted, similarly to

that observed at 200 K. As a result, two of the 5-7 pair defects were formed, as shown in Fig. 3(h). The average temperature was estimated to be 3121 K. At this initial temperature, the number of emitted atoms increased, compared with the simulation at 200 K. Correspondingly, the distance between seven-membered rings was larger than that observed at 200 K [compare Figs. 3(b) and 3(h)].

In the case of an initial temperature of 2600 K, a hole appeared inside the arc by bond breakage and, after approximately 1.0–2.0 ps, was closed by bond reconstruction. On the other hand, a bond rotation of 90 degrees formed a
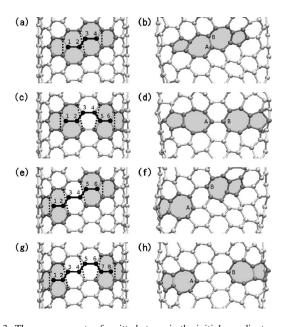

FIG. 3. The arrangements of emitted atoms in the initial coordinates and the structures of the coupled 5-7 pair defects viewed from inside the arc. The emitted atoms are numbered and denoted in black. The atoms which constitute these defects are denoted in gray. (a) The arrangement of the four emitted atoms, and (b) the coupled 5-7 pair defects formed by a four-atom emission. The arrangements for six-atom emissions, (c) one and (e) the other. The resulting defect structures of six-atom emission are shown in (d) and (f), respectively. The case of eight-atom emission is shown in (g) and (h).
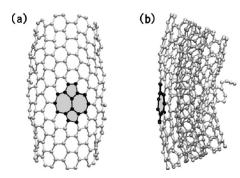
(a)   **(b)**

FIG. 4. SW defect on the outside of the arc (a) formed at 2600 K, and its side view (b). The atoms which constitute the defect are indicated in black. The inner tube is not represented in (a) for clarification.

Stone–Wales (SW) defect[25] on the outside of the arc, as shown in Fig. 4. The average temperature in this simulation was 3592 K. In the case of an initial temperature of 4000 K, a large hole appeared at the inside of the arc and the wall was fractured. Furthermore, as a result of bond breakage of the inner tube, a bond was formed between the inner and outer tubes. On the outside of the arc, the atoms were emitted and a hole appeared. The frequency of bond breakage and rebonding was increased as the initial temperature increased. Hereafter, all the temperatures indicate respective initial temperatures.

B. Details of simulations

1. Emission of clusters

Figure 2 shows the process of atom emission in the simulation at an initial temperature of 200 K. The emitted atoms are highlighted in black, and the outer and inner tubes are denoted by light and dark gray, respectively. At the beginnings, several bonds along the axis of the tube were broken at the inside of the arc [Fig. 2(a)]. These bonds were broken successively and the hole appeared along the circumference of the tube [Fig. 2(b)]. After that, the hole began to close by atomic rearrangement. In this process, the atoms denoted by black in Fig. 2 were pushed out of the tube [Fig. 2(c)]. As a result, a cluster of four atoms in the straight-chain were emitted and the hole was completely closed, resulting in the formation of a 5-7 pair couple defect [Fig. 2(d)] inside the arc of the outer tube. This defect was thermally stable until 3.0 ps and bond breakage did not occur.

Similar simulations were carried out for SWNTs; however, it was found that the emission of atoms did not occur. Since the inside of a SWNT is empty, the SWNT collapsed along the circumference direction, and this result is consistent with the previous work.[6] In contrast to SWNTs, DWNTs did not collapse due to the existence of the inner tube. As a result, the atoms of the outer tube were pushed out by the inner tube and were then emitted.

The tight-binding model used in this study does not describe van der Waals interactions of the interlayer between graphene sheets. Therefore, the interwall interactions of DWNTs cannot be described completely. Atom emission occurs when the wall of the outer tube becomes close to that of the inner tube, and in this situation, the repulsion between the walls becomes greater than the van der Waals interac-

TABLE I. The number of emitted atoms depending on an initial temperature T. Each column corresponds to three sets of simulations. In each simulation set, the same random seed was used for the initial atomic velocity. In parentheses the total number of atoms which were ejected from the wall of the nanotube is denoted.

T (K)	Number of emitted atoms		
	Seed 1	Seed 2	Seed 3
200	4	2	-
400	-	-	-
600	-	-	2
800	6	-	-
1000	-	-	-
1200	6	5 (10)	2
1400	8	2 (8)	6
1600	6	7 (10)	2
1800	6	5 (10)	-
2000	8	5	4

tions. However, since atom emission occurs at high temperatures, the contribution of van der Waals forces would be small compared with the kinetic energy of atomic motions. Contrastively, phenomena which occur in the intralayer, such as the rearrangement of bonds and the formation of SW defects, may be represented adequately by the tight-binding model;[26] therefore, phenomena such as atom emission and the formation of 5-7 pair couple defects may also be well represented.

2. Formation of defects

Figures 3(a) and 3(b) show the arrangement of emitted atoms in the initial coordination and final coordination for 5-7 pair couple defects. In Fig. 3(a), the bonds located around the cluster of black atoms were broken during emission and the created bonds between the atoms are indicated by the dashed lines and were formed after emitting the atoms indicated in black. Finally two five- and seven-membered pair rings were formed as shown in Fig. 3(b).

In order to investigate phenomena occurring for an initial temperature, we performed a number of simulations at different temperatures in iterations of 200 K over a range from 0 to 5000 K. From 200 to 2000 K, 5-7 pair defect couples were formed with atom emission. In Table I, the second column (seed 1) summarizes the number of emitted atoms in these simulations. From the second column in Table I, it is shown that from 200 to 1000 K atom emission occurred depending on the temperature. On the other hand, from 1200 to 2000 K atom emission always occurred. At temperatures less than 2000 K, an interesting phenomenon occurred mainly at the inside of the arc, whereby compression was imposed under bending deformation. From 2200 to 3000 K, thermal vibration of the atoms became intense and various phenomena such as the formation of 5–7 pair couple defects and five- and seven-membered rings were found, in addition to the formation of holes and emission of atoms from inside the arc. Formed holes were closed by atomic rearrangement. Structural defects such as five- and seven-membered rings and the SW defect were formed on the outside of the arc. From 3200 to 5000 K, vibration of atoms

became more intense and even on the outside of the arc, the hole was no longer closed. The number of emitted atoms and the frequency of bond breakages and rebondings increased with increasing temperature. At temperatures higher than 3200 K, breakage was observed in both the outer and inner tubes.

At temperatures higher than 3200 K, SW defects were formed on the outside of the arc as shown in Fig. 4, and these results are in agreement with results obtained by Nardelli *et al.*[7] They found that nanotubes that contain SW defects are energetically preferred in a uniformly stretched tube which has a strain larger than the 5% strain, while in our simulation the outside of the arc was stretched by 18% at the initial condition of bending.

3. Structure of defects

We observed the emission of clusters with four-, six-, and eight-atoms, resulting in the production of 5-7 pair couple defects, and the geometry of the 5-7 pair defects was dependent on the number and configuration of the emitted atoms. Figure 3 shows the arrangements of emitted atoms in the initial coordinates and the structures of the 5–7 pair couple defects. In Fig. 3(a), at an initial temperature of 200 K, four black atoms were emitted, and the 5–7 pair couple defects, in which two seven-membered rings share a bond (denoted by A and B in figure), were formed as shown in Fig. 3(b).

At temperatures of 800, 1200, and 1600 K, six atoms were emitted, as shown in the column of seed 1 in Table I. At all three temperatures, the arrangements of emitted atoms were similar to that shown in Fig. 3(c). The resulting defect is shown in Fig. 3(d), in which the 5-7 pair defects are separated by a single (AB) bond. Another type of six-atom emission was observed at 1800 K, as shown in Figs. 3(e) and 3(f). In this case, the 5-7 pair defects were separated by a single six-membered ring. Although the resulting configurations vary depending upon the type of six-atom emission [(d) and (f)], in both cases the 5-7 pair defects are separated by an array of the hexagonal rings aligned along the axial direction of the tube.

At 1400 and 2000 K, eight-atom emissions occurred [Figs. 3(g) and 3(h)]. In the observed defect, the 5-7 pair defects are separated by a double array of hexagonal rings, as shown in Fig. 3(h). The distance between the 5-7 pair defects increases with increasing number of emitted atoms.

As a result of atom emission, the number of six-membered rings on the inside of the arc decreased. When a $2n$-atom emission occurs, the number of rings are decreased by n from the original configuration of the hexagonal network. Due to the loss of aligned atoms, 5-7 pair defects are located in the dislocation core, and this decrease relaxes the stress raised by the bending deformation. The resulting nanotube, which includes the 5-7 pair couple defects, has no dangling bonds, and all bonds except the bonds located on each end of the tube are sp^2-like bonds. This rebonding resulted in stabilization of the nanotube with the defects.
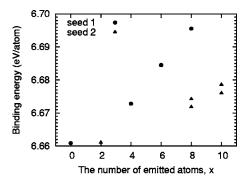

FIG. 5. The binding energy of the stable structure in seed 1 (circle) and seed 2 (triangle) represented as a function of the number of emitted atoms (x) under bending deformation. The structure in seed 1 has 5-7 pair couple defects. For $x=2$, the structure has a 5-8-5 defect.

4. Stability of defects

In order to investigate the stability of the 5-7 pair couple defects, we optimized the structures of the nanotube having the defect by fixing the coordinates of the atoms at both ends of the tubes. The binding energies of the optimized structures were plotted as a function of the number of emitted atoms in Fig. 5. The two energies of six-atom emission, which were obtained from the configurations in Figs. 3(d) and 3(f), were almost equal. Figure 5 shows that the binding energy per atom increases with the number of emitted atoms. The optimized structure for the nanotube obtained from the eight-atom emission is presented in Fig. 3(h). The outline shape of the nanotube at the inside of the arc is smooth, as shown in Fig. 6(b), implying tube stability. Structural optimization was also carried out for nanotubes without defects [see Fig. 1(b)], and the optimized structure was shown to obtain a buckle as shown in Fig. 6(a). As a result, the binding energy per atom of the buckle structure without defects was lower than that of the optimized structure by a difference of 0.04 eV/atom with the 5-7 pair couple defects.

5. Simulations of different conditions

In order to investigate dependence on the curvature radius of the arc in the initial coordinate, simulations under various curvature radii were performed. In these simulations the temperature range was from 0 to 4000 K, proceeding by iterations of 1000 K. The main observed phenomena of the
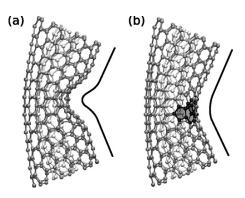

FIG. 6. The optimized structures under bending deformation for nondefect (a) and defect (b) nanotubes. The latter was obtained from the resulting structure of an eight-atom emission. In (b), the number of the hexagonal rings is decreased inside of the arc compared with (a).

TABLE II. Noteworthy phenomena which occurred at various curvature radii R for the arc with the bending angles θ. Bending angles are calculated from curvature radii.

R (Å)	θ (degree)	Phenomena
20	67	Breakdown of nanotubes
30	45	Atom emission, 5-7 pair couple defects, SW defect
35	38	Atom emission, 5-7 pair couple defects, Interstitial defect, SW defect
40	34	Formation of interstitial defect
50	27	Thermal vibration
60	22	Thermal vibration

simulations are summarized in Table II with the bending angles indicated. When the curvature radii were 60 Å and 50 Å, only thermal vibrations occurred, although the initial temperature increased up to 4000 K. In the case of 40 Å, interstitials between the walls of the DWNT were formed at 4000 K. One of the typical geometries for interstitials is shown in Fig. 7. Noteworthy phenomena such as atom emission, formation of 5-7 pair couple defects, and SW defects occurred in the curvature radius range of 35–30 Å. In the case of 20 Å, breakdown of the nanotube was caused by large distortions of the nanotube.

All of the above simulations used the same seed (seed 1) in the random number generator for the initial atomic velocities. In order to see dependencies on the initial velocity distribution, which may correspond to thermal fluctuation under bending deformation, two additional sets of simulations were performed using different seeds (seeds 2 and 3). The effect of the initial temperatures was investigated stepwise in increments of 200 K, from 200 to 2000 K.

The numbers of emitted atoms in these simulations are summarized in the third and fourth columns of Table I. In the one set of simulations (seed 2, the third column of Table I), atom emission did not occur at temperatures less than or equal to 1000 K, except at 200 K. At 200 K, two atoms were emitted and a 5-8-5 defect was formed, as shown in Fig. 8(a). The formation of this defect (lack of two atoms) was observed in previous simulations of SWNT.[27] At 400 and 600 K, only thermal vibrations occurred and at 800 and 1000 K, SW defects were formed on the inside of the arc.

From 1200 to 2000 K in seed 2, atom emissions were observed in all simulations. At 1200 K, five atoms were emitted and another five atoms were ejected from the wall of
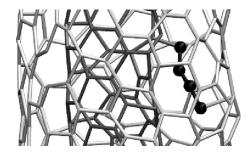

FIG. 7. Snapshot of the typical geometry for interstitials (black atoms) from a simulation with a curvature radius of 40 Å at 4000 K.
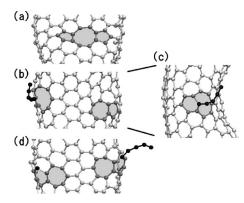

FIG. 8. The structures of the defects formed in the simulations of seed 2. Those atoms which constituted the defects and those which were ejected but remained attached to the wall of the tube are denoted in gray and in black, respectively. (a) The 5-8-5 defect was formed by a two-atom emission at 200 K. A 10-atom loss formed an incomplete 5-7 pair couple defect (b), and side view (c) at 1200 K. (d) An incomplete 5-7 pair couple defect was formed at 1400 K.

the tube on the inside of the arc. The latter five atoms formed a chain and were ejected but remained attached to the surface of the nanotube. As a result, a defect was formed but it was not of the 5-7 pair type, and we refer to this defect as an incomplete 5-7 pair couple defect, as shown in Figs. 8(b) and 8(c). Although we carried out successive simulations at 7 ps, the chain still existed and the atoms were not emitted. In this simulation, the wall of the nanotube lost 10 atoms in total. In the parentheses of Table I the total number of lost atoms from the wall are denoted. In this type of defect, the 5-7 pair couple defects are separated by a triple array of hexagonal rings.

At 1400 K, the wall of the nanotube lost eight atoms in total. Two atoms were emitted, five atoms formed a chain, and the other atom was similar to an adatom. In the wall, incomplete 5-7 pair couple defects were formed, as shown in Fig. 8(d), and as shown in the figure, the right-side 5-7 pair has a chain and the left-side 5-7 pair has a single atom which was ejected from the wall. Except for the presence of ejected but attached atoms, the defect is very similar to that of the eight-atom emission shown in Fig. 3(h). The arrangement of lost atoms is different from the simulations of seed 1 at 1400 and 2000 K [see Fig. 3(g)]. At 1600 and 1800 K, 10-atom loss resulted in an incomplete 5-7 pair couple defect. The resulting defects and the arrangements of lost atoms were similar to that which occurred at 1200 K in seed 2, except that the chain length was different [refer to Figs. 8(b) and 8(c)]. In seed 2, many of the resulting defects may be considered to be variations of a 5-7 pair couple defect.

At 2000 K, various noteworthy phenomena were observed such as atom emission and the formation of five-, seven-, and eight-membered rings and interstitials on the inside of the arc. The wall on the inside of the arc exhibited an amorphous-like two-dimensional structure. On the outside of the arc, SW defects were formed. These results are similar to those of the simulations in seed 1, where the temperature exceeded 2200 K.

The resulting configurations generated by seed 2 have been also used to evaluate binding energies which are presented in Fig. 5. The defects generated at temperatures
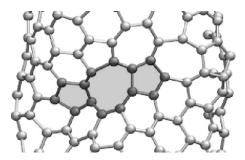
FIG. 9. The defect structure formed at 1400 K in the simulations of seed 3.

higher than 1000 K may release strain energies, but the quantities of energy are lower than that of seed 1 due to the incompleteness of the couple defects in seed 2. It is interesting that we observed linear dependences of binding energy with respect to the number of emitted atoms (x), for example, the data at $x=2$ of seed 2 and $x=4,6,8$ of seed 1 in Fig. 5.

In the other set of simulations (seed 3, the fourth column of Table I), similar to the cases of seeds 1 and 2, atom emission did not occur at temperatures less than or equal to 1000 K, except for 600 K. Some defects generated at 600, 800, 1200, and 1400 K could be related to variations of the 5-8-5 defect, which is shown in Fig. 8(a). One of the resulting arrangements at 1400 K is displayed in Fig. 9, whose 5-8-5 defect is connected with a 5-7 pair couple defect which was abundantly produced in the cases of seeds 1 and 2. At other temperatures higher than 1000 K in seed 3, there are complex defects related to atom emission, the formation of 5-, 7-, and 8-membered rings, interstitials, and bond formations between inner and outer walls.

The binding energy of the 5-8-5 defect, as shown at $x=2$ in Fig. 5, is comparable to the value of the nondefect tube ($x=0$), indicating little energy gain with a 5-8-5 defect. This defect minimally released the strain induced by the bending deformation, and this may be attributed to the planar structure of the 5-8-5 defect. It was also observed in another case whereby the binding energy of the resulting arrangement amounted to 6.673 eV/atom (Fig. 9), which was comparable to that of the arrangement presented in Fig. 3 ($x=4$ in Fig. 5).

The three sets of simulations, each with different initial velocity distributions, showed that atom emission depended on the initial velocity distributions at an initial temperature from 200 to 1000 K. From 1200 to 2000 K, atom emission occurred normally without dependence on the initial velocity distribution. In the simulations of seeds 1 and 2, the resulting defects were related to the 5-7 pair couple defect, while in seed 3 some of the resulting defects were related to the 5-8-5 defect. The latter defect may relax the structure only in a small area, as in the case of a "point defect," and the 5–7 pair couple defects may release stresses to a larger area by a "dislocation" type of effect. The latter may also be adjustable due to the changes in the distances between the 5-7 pair couple defects.

C. Comparison with similar defects in carbon materials

The results of our simulations predict the existence of 5-7 pair couple defects in nanotubes. Recently, a single 5-7

pair defect formed by emission of carbon clusters in a graphene layer was observed by high-resolution transmission electron microscopy (HR-TEM).[28] It was reported that during the formation of this topological defect, an elastic deformation or a bending of the graphene layer was observed in the time-sequential HR-TEM image. Niwase has proposed a model of pair defects in the basal plane of graphite under irradiation,[29] in which the hexagonal rings reappear between the pair defects after the relaxation of the cluster vacancies. The structures of those defects are similar to the 5-7 pair couple defects. The 5-7 pair couple defects may be formed by a lack of atoms in a synthesized nanotube. Therefore it is possible that these defects may be formed by irradiation of nanotubes. Several groups have also reported a lack of atoms in nanotubes that were subjected to irradiation.[30–32] Recently the nanotube defects were studied experimentally,[33] but further experimental work is required to confirm the presence of these defects.

IV. SUMMARY

Simulations of DWNTs under bending deformation by using the tight-binding molecular dynamics method were carried out and bond breakage, rebondings, atom emissions, and the formation of defects were observed. At low temperatures, the inner tube maintained its original carbon network and noteworthy phenomena were observed only in the outer tube. These behaviors differ from the case of SWNTs under bending deformation. After an atom emission from the outer tube, 5-7 pair couple defects were observed in the outer tubes and these defects stabilized the system under bending deformation. The structure of the couple defect depends on the number and the arrangement of the cluster of emitted atoms, and our results imply that the couple defects are one of the origins for the plastic deformation observed in DWNTs. The defects obtained at moderate temperatures (≤ 2000 K) in the simulations were discussed as variants of ideal 5-7 pair couple defects and an ideal 5-8-5 defect. SW defects were observed on the outside of the tubes where tension was imposed. Detailed defect observations on both SWNTs and MWNTs, as has been performed on defect-induced graphenes, is eagerly awaited.

[1]S. Iijima, Nature (London) **354**, 56 (1991).
[2]J. F. Despres, E. Daguerre, and K. Lafdi, Carbon **33**, 87 (1995).
[3]S. Iijima, C. Brabec, A. Maiti, and J. Bernholc, J. Chem. Phys. **104**, 2089 (1996).
[4]B. I. Yakobson, C. J. Brabec, and J. Bernholc, Phys. Rev. Lett. **76**, 2511 (1996).
[5]M. R. Falvo, G. J. Clary, R. M. I. Taylor, V. Chi, F. P. J. Brooks, S. Washburn, and R. Superfine, Nature (London) **389**, 582 (1997).
[6]M. Huhtala, A. Kuronen, and K. Kaski, Int. J. Mod. Phys. C **15**, 517

(2004).

[7]M. B. Nardelli, B. I. Yakobson, and J. Bernholc, Phys. Rev. B **57**, R4277 (1998).

[8]M. B. Nardelli, J. L. Fattebert, D. Orlikowski, C. Roland, Q. Zhao, and J. Bernholc, Carbon **38**, 1703 (2000).

[9]T. Dumitrica and B. I. Yakobson, Appl. Phys. Lett. **84**, 2775 (2004).

[10]S. Bandow, M. Takizawa, K. Hirahara, M. Yudasaka, and S. Iijima, Chem. Phys. Lett. **337**, 48 (2001).

[11]J. Wei, L. Ci, B. Jiang, Y. Li, X. Zhang, H. Zhu, C. Xu, and D. Wu, J. Mater. Chem. **13**, 1340 (2003).

[12]S. Lyu, B. Liu, C. Lee, H. Kang, C. Yang, and C. Park, Chem. Mater. **15**, 3951 (2003).

[13]T. Hiraoka, T. Kawakubo, J. Kimura, R. Taniguchi, A. Okamoto, T. Okazaki, T. Sugai, Y. Ozeki, M. Yoshikawa, and H. Shinohara, Chem. Phys. Lett. **382**, 679 (2003).

[14]E. Flahaut, R. Bacsa, A. Peigney, and C. Laurent, Chem. Commun. **12**, 1442 (2003).

[15]S. Lyu, B. Liu, S. Lee, C. Park, H. Kang, C. Yang, and C. Lee, J. Phys. Chem. B **108**, 2192 (2004).

[16]Y. Nakayama, A. Nagataki, O. Sekane, X. Cai, and S. Akita, Jpn. J. Appl. Phys. **44**, L720 (2005).

[17]J. Han, M. Anantram, R. Jaffe, J. Kong, and H. Dai, Phys. Rev. B **57**, 14983 (1998).

[18]H. Mori, S. Ogata, J. Li, S. Akita, and Y. Nakayama, Phys. Rev. B **74**, 165418 (2006).

[19]R. Saito, R. Matsuo, T. Kimura, G. Dresselhaus, and M. Dresselhaus, Chem. Phys. Lett. **348**, 187 (2001).

[20]X. Zhao, Y. Liu, S. Inoue, T. Suzuki, R. Jones, and Y. Ando, Phys. Rev. Lett. **92**, 125502 (2004).

[21]C. H. Xu, C. Z. Wang, C. T. Chan, and K. M. Ho, J. Phys.: Condens. Matter **4**, 6047 (1992).

[22]R. Car and M. Parrinello, Phys. Rev. Lett. **55**, 2471 (1985).

[23]M. C. Payne, M. P. Teter, D. C. Allan, T. A. Arias, and J. D. Joannopoulos, Rev. Mod. Phys. **64**, 1045 (1992).

[24]L. Verlet, Phys. Rev. **159**, 98 (1967).

[25]A. Stone and D. Wales, Chem. Phys. Lett. **128**, 501 (1986).

[26]V. H. Crespi, L. X. Benedict, M. L. Cohen, and S. G. Louie, Phys. Rev. B **53**, R13303 (1996).

[27]M. Sammalkorpi, A. Krasheninnikov, A. Kuronen, K. Nordlund, and K. Kaski, Phys. Rev. B **70**, 245416 (2004).

[28]A. Hashimoto, K. Suenaga, A. Gloter, K. Urita, and S. Iijima, Nature (London) **430**, 870 (2004).

[29]K. Niwase, Mater. Sci. Eng., A **400-401**, 101 (2005).

[30]A. Kis, G. Csanyi, J.-P. Salvetat, T.-N. Lee, E. Couteau, A. J. Kulik, W. Benoit, J. Brugger, and L. Forro, Nat. Mater. **3**, 153 (2004).

[31]B. W. Smith and D. E. Luzzi, J. Appl. Phys. **90**, 3509 (2001).

[32]A. Krasheninnikov and K. Nordlund, Nucl. Instrum. Methods Phys. Res. B **216**, 355 (2004).

[33]T. Uchida, M. Tachibana, and K. Kojima, J. Appl. Phys. **101**, 084313 (2007).